BABAR-CONF-02/04
SLAC-PUB-9171
hep-ex/0203034
March 2002

A Measurement of the $B^0 \to J/\psi\pi^+\pi^-$ Branching Fraction

The *BABAR* Collaboration

Abstract

We present a preliminary measurement of the branching fraction for the decay of the neutral B meson into the final state $J/\psi\pi^+\pi^-$. The data set contains approximately 56 million $B\overline{B}$ pairs produced at the $\Upsilon(4S)$ resonance and recorded by the *BABAR* detector at the PEP-II e^+e^- collider. The result of this analysis is $\mathcal{B}(B^0 \to J/\psi\pi^+\pi^-) = (5.0 \pm 0.7 \pm 0.6)\times 10^{-5}$, where the first error is statistical and the second is systematic.

Presented at the XXXVIIth Rencontres de Moriond on QCD and Hadronic Interactions,
3-16—3/23/2002, Les Arcs, Savoie, France

Stanford Linear Accelerator Center, Stanford University, Stanford, CA 94309

Work supported in part by Department of Energy contract DE-AC03-76SF00515.

The *BABAR* Collaboration,

B. Aubert, D. Boutigny, J.-M. Gaillard, A. Hicheur, Y. Karyotakis, J. P. Lees, P. Robbe, V. Tisserand, A. Zghiche

Laboratoire de Physique des Particules, F-74941 Annecy-le-Vieux, France

A. Palano, A. Pompili

Università di Bari, Dipartimento di Fisica and INFN, I-70126 Bari, Italy

G. P. Chen, J. C. Chen, N. D. Qi, G. Rong, P. Wang, Y. S. Zhu

Institute of High Energy Physics, Beijing 100039, China

G. Eigen, I. Ofte, B. Stugu

University of Bergen, Inst. of Physics, N-5007 Bergen, Norway

G. S. Abrams, A. W. Borgland, A. B. Breon, D. N. Brown, J. Button-Shafer, R. N. Cahn, E. Charles, M. S. Gill, A. V. Gritsan, Y. Groysman, R. G. Jacobsen, R. W. Kadel, J. Kadyk, L. T. Kerth, Yu. G. Kolomensky, J. F. Kral, C. LeClerc, M. E. Levi, G. Lynch, L. M. Mir, P. J. Oddone, M. Pripstein, N. A. Roe, A. Romosan, M. T. Ronan, V. G. Shelkov, A. V. Telnov, W. A. Wenzel

Lawrence Berkeley National Laboratory and University of California, Berkeley, CA 94720, USA

T. J. Harrison, C. M. Hawkes, D. J. Knowles, S. W. O'Neale, R. C. Penny, A. T. Watson, N. K. Watson

University of Birmingham, Birmingham, B15 2TT, United Kingdom

T. Deppermann, K. Goetzen, H. Koch, B. Lewandowski, K. Peters, H. Schmuecker, M. Steinke

Ruhr Universität Bochum, Institut für Experimentalphysik 1, D-44780 Bochum, Germany

N. R. Barlow, W. Bhimji, N. Chevalier, P. J. Clark, W. N. Cottingham, B. Foster, C. Mackay, F. F. Wilson

University of Bristol, Bristol BS8 1TL, United Kingdom

K. Abe, C. Hearty, T. S. Mattison, J. A. McKenna, D. Thiessen

University of British Columbia, Vancouver, BC, Canada V6T 1Z1

S. Jolly, A. K. McKemey

Brunel University, Uxbridge, Middlesex UB8 3PH, United Kingdom

V. E. Blinov, A. D. Bukin, D. A. Bukin, A. R. Buzykaev, V. B. Golubev, V. N. Ivanchenko, A. A. Korol, E. A. Kravchenko, A. P. Onuchin, S. I. Serednyakov, Yu. I. Skovpen, A. N. Yushkov

Budker Institute of Nuclear Physics, Novosibirsk 630090, Russia

D. Best, M. Chao, D. Kirkby, A. J. Lankford, M. Mandelkern, S. McMahon, D. P. Stoker

University of California at Irvine, Irvine, CA 92697, USA

K. Arisaka, C. Buchanan, S. Chun

University of California at Los Angeles, Los Angeles, CA 90024, USA

D. B. MacFarlane, S. Prell, Sh. Rahatlou, G. Raven, V. Sharma

University of California at San Diego, La Jolla, CA 92093, USA

C. Campagnari, B. Dahmes, P. A. Hart, N. Kuznetsova, S. L. Levy, O. Long, A. Lu, M. A. Mazur, J. D. Richman, W. Verkerke

University of California at Santa Barbara, Santa Barbara, CA 93106, USA

J. Beringer, A. M. Eisner, M. Grothe, C. A. Heusch, W. S. Lockman, T. Pulliam, T. Schalk, R. E. Schmitz, B. A. Schumm, A. Seiden, M. Turri, W. Walkowiak, D. C. Williams, M. G. Wilson

University of California at Santa Cruz, Institute for Particle Physics, Santa Cruz, CA 95064, USA

E. Chen, G. P. Dubois-Felsmann, A. Dvoretskii, D. G. Hitlin, S. Metzler, J. Oyang, F. C. Porter, A. Ryd, A. Samuel, S. Yang, R. Y. Zhu

California Institute of Technology, Pasadena, CA 91125, USA

S. Jayatilleke, G. Mancinelli, B. T. Meadows, M. D. Sokoloff

University of Cincinnati, Cincinnati, OH 45221, USA

T. Barillari, P. Bloom, W. T. Ford, U. Nauenberg, A. Olivas, P. Rankin, J. Roy, J. G. Smith, W. C. van Hoek, L. Zhang

University of Colorado, Boulder, CO 80309, USA

J. Blouw, J. L. Harton, M. Krishnamurthy, A. Soffer, W. H. Toki, R. J. Wilson, J. Zhang

Colorado State University, Fort Collins, CO 80523, USA

T. Brandt, J. Brose, T. Colberg, M. Dickopp, R. S. Dubitzky, A. Hauke, E. Maly, R. Müller-Pfefferkorn, S. Otto, K. R. Schubert, R. Schwierz, B. Spaan, L. Wilden

Technische Universität Dresden, Institut für Kern- und Teilchenphysik, D-01062 Dresden, Germany

D. Bernard, G. R. Bonneaud, F. Brochard, J. Cohen-Tanugi, S. Ferrag, S. T'Jampens, Ch. Thiebaux, G. Vasileiadis, M. Verderi

Ecole Polytechnique, LLR, F-91128 Palaiseau, France

A. Anjomshoaa, R. Bernet, A. Khan, D. Lavin, F. Muheim, S. Playfer, J. E. Swain, J. Tinslay

University of Edinburgh, Edinburgh EH9 3JZ, United Kingdom

M. Falbo

Elon University, Elon University, NC 27244-2010, USA

C. Borean, C. Bozzi, L. Piemontese

Università di Ferrara, Dipartimento di Fisica and INFN, I-44100 Ferrara, Italy

E. Treadwell

Florida A&M University, Tallahassee, FL 32307, USA

F. Anulli,[1] R. Baldini-Ferroli, A. Calcaterra, R. de Sangro, D. Falciai, G. Finocchiaro, P. Patteri, I. M. Peruzzi,[2] M. Piccolo, Y. Xie, A. Zallo

Laboratori Nazionali di Frascati dell'INFN, I-00044 Frascati, Italy

S. Bagnasco, A. Buzzo, R. Contri, G. Crosetti, M. Lo Vetere, M. Macri, M. R. Monge, S. Passaggio, F. C. Pastore, C. Patrignani, E. Robutti, A. Santroni, S. Tosi

Università di Genova, Dipartimento di Fisica and INFN, I-16146 Genova, Italy

[1]Also with Università di Perugia, I-06100 Perugia, Italy
[2]Also with Università di Perugia, I-06100 Perugia, Italy

M. Morii

Harvard University, Cambridge, MA 02138, USA

R. Bartoldus, R. Hamilton, U. Mallik

University of Iowa, Iowa City, IA 52242, USA

J. Cochran, H. B. Crawley, J. Lamsa, W. T. Meyer, E. I. Rosenberg, J. Yi

Iowa State University, Ames, IA 50011-3160, USA

G. Grosdidier, A. Höcker, H. M. Lacker, S. Laplace, F. Le Diberder, V. Lepeltier, A. M. Lutz, S. Plaszczynski, M. H. Schune, S. Trincaz-Duvoid, G. Wormser

Laboratoire de l'Accélérateur Linéaire, F-91898 Orsay, France

R. M. Bionta, V. Brigljević , D. J. Lange, M. Mugge, K. van Bibber, D. M. Wright

Lawrence Livermore National Laboratory, Livermore, CA 94550, USA

A. J. Bevan, J. R. Fry, E. Gabathuler, R. Gamet, M. George, M. Kay, D. J. Payne, R. J. Sloane, C. Touramanis

University of Liverpool, Liverpool L69 3BX, United Kingdom

M. L. Aspinwall, D. A. Bowerman, P. D. Dauncey, U. Egede, I. Eschrich, G. W. Morton, J. A. Nash, P. Sanders, D. Smith

University of London, Imperial College, London, SW7 2BW, United Kingdom

J. J. Back, G. Bellodi, P. Dixon, P. F. Harrison, R. J. L. Potter, H. W. Shorthouse, P. Strother, P. B. Vidal

Queen Mary, University of London, E1 4NS, United Kingdom

G. Cowan, S. George, M. G. Green, A. Kurup, C. E. Marker, T. R. McMahon, S. Ricciardi, F. Salvatore, G. Vaitsas

University of London, Royal Holloway and Bedford New College, Egham, Surrey TW20 0EX, United Kingdom

D. Brown, C. L. Davis

University of Louisville, Louisville, KY 40292, USA

J. Allison, R. J. Barlow, J. T. Boyd, A. C. Forti, F. Jackson, G. D. Lafferty, N. Savvas, J. H. Weatherall, J. C. Williams

University of Manchester, Manchester M13 9PL, United Kingdom

A. Farbin, A. Jawahery, V. Lillard, J. Olsen, D. A. Roberts, J. R. Schieck

University of Maryland, College Park, MD 20742, USA

G. Blaylock, C. Dallapiccola, K. T. Flood, S. S. Hertzbach, R. Kofler, V. B. Koptchev, T. B. Moore, H. Staengle, S. Willocq

University of Massachusetts, Amherst, MA 01003, USA

B. Brau, R. Cowan, G. Sciolla, F. Taylor, R. K. Yamamoto

Massachusetts Institute of Technology, Laboratory for Nuclear Science, Cambridge, MA 02139, USA

M. Milek, P. M. Patel

McGill University, Montréal, QC, Canada H3A 2T8

F. Palombo, C. Vite

Università di Milano, Dipartimento di Fisica and INFN, I-20133 Milano, Italy

J. M. Bauer, L. Cremaldi, V. Eschenburg, R. Kroeger, J. Reidy, D. A. Sanders, D. J. Summers

University of Mississippi, University, MS 38677, USA

C. Hast, J. Y. Nief, P. Taras

Université de Montréal, Laboratoire René J. A. Lévesque, Montréal, QC, Canada H3C 3J7

H. Nicholson

Mount Holyoke College, South Hadley, MA 01075, USA

C. Cartaro, N. Cavallo,[3] G. De Nardo, F. Fabozzi, C. Gatto, L. Lista, P. Paolucci, D. Piccolo, C. Sciacca

Università di Napoli Federico II, Dipartimento di Scienze Fisiche and INFN, I-80126, Napoli, Italy

J. M. LoSecco

University of Notre Dame, Notre Dame, IN 46556, USA

J. R. G. Alsmiller, T. A. Gabriel

Oak Ridge National Laboratory, Oak Ridge, TN 37831, USA

J. Brau, R. Frey, E. Grauges , M. Iwasaki, C. T. Potter, N. B. Sinev, D. Strom

University of Oregon, Eugene, OR 97403, USA

F. Colecchia, F. Dal Corso, A. Dorigo, F. Galeazzi, M. Margoni, M. Morandin, M. Posocco, M. Rotondo, F. Simonetto, R. Stroili, E. Torassa, C. Voci

Università di Padova, Dipartimento di Fisica and INFN, I-35131 Padova, Italy

M. Benayoun, H. Briand, J. Chauveau, P. David, Ch. de la Vaissière, L. Del Buono, O. Hamon, Ph. Leruste, J. Ocariz, M. Pivk, L. Roos, J. Stark

Universités Paris VI et VII, Lab de Physique Nucléaire H. E., F-75252 Paris, France

P. F. Manfredi, V. Re, V. Speziali

Università di Pavia, Dipartimento di Elettronica and INFN, I-27100 Pavia, Italy

E. D. Frank, L. Gladney, Q. H. Guo, J. Panetta

University of Pennsylvania, Philadelphia, PA 19104, USA

C. Angelini, G. Batignani, S. Bettarini, M. Bondioli, F. Bucci, E. Campagna, M. Carpinelli, F. Forti, M. A. Giorgi, A. Lusiani, G. Marchiori, F. Martinez-Vidal, M. Morganti, N. Neri, E. Paoloni, M. Rama, G. Rizzo, F. Sandrelli, G. Simi, G. Triggiani, J. Walsh

Università di Pisa, Scuola Normale Superiore and INFN, I-56010 Pisa, Italy

M. Haire, D. Judd, K. Paick, L. Turnbull, D. E. Wagoner

Prairie View A&M University, Prairie View, TX 77446, USA

J. Albert, P. Elmer, C. Lu, V. Miftakov, S. F. Schaffner, A. J. S. Smith, A. Tumanov, E. W. Varnes

Princeton University, Princeton, NJ 08544, USA

[3]Also with Università della Basilicata, I-85100 Potenza, Italy

F. Bellini, G. Cavoto, D. del Re, R. Faccini,[4] F. Ferrarotto, F. Ferroni, M. A. Mazzoni, S. Morganti, G. Piredda, M. Serra, C. Voena

Università di Roma La Sapienza, Dipartimento di Fisica and INFN, I-00185 Roma, Italy

S. Christ, R. Waldi

Universität Rostock, D-18051 Rostock, Germany

T. Adye, N. De Groot, B. Franek, N. I. Geddes, G. P. Gopal, S. M. Xella

Rutherford Appleton Laboratory, Chilton, Didcot, Oxon, OX11 0QX, United Kingdom

R. Aleksan, S. Emery, A. Gaidot, S. F. Ganzhur, P.-F. Giraud, G. Hamel de Monchenault, W. Kozanecki, M. Langer, G. W. London, B. Mayer, B. Serfass, G. Vasseur, Ch. Yèche, M. Zito

DAPNIA, Commissariat à l'Energie Atomique/Saclay, F-91191 Gif-sur-Yvette, France

M. V. Purohit, A. W. Weidemann, F. X. Yumiceva

University of South Carolina, Columbia, SC 29208, USA

I. Adam, D. Aston, N. Berger, A. M. Boyarski, G. Calderini, M. R. Convery, D. P. Coupal, D. Dong, J. Dorfan, W. Dunwoodie, R. C. Field, T. Glanzman, S. J. Gowdy, T. Haas, T. Hadig, V. Halyo, T. Himel, T. Hryn'ova, M. E. Huffer, W. R. Innes, C. P. Jessop, M. H. Kelsey, P. Kim, M. L. Kocian, U. Langenegger, D. W. G. S. Leith, S. Luitz, V. Luth, H. L. Lynch, H. Marsiske, S. Menke, R. Messner, D. R. Muller, C. P. O'Grady, V. E. Ozcan, A. Perazzo, M. Perl, S. Petrak, H. Quinn, B. N. Ratcliff, S. H. Robertson, A. Roodman, A. A. Salnikov, T. Schietinger, R. H. Schindler, J. Schwiening, A. Snyder, A. Soha, S. M. Spanier, J. Stelzer, D. Su, M. K. Sullivan, H. A. Tanaka, J. Va'vra, S. R. Wagner, M. Weaver, A. J. R. Weinstein, W. J. Wisniewski, D. H. Wright, C. C. Young

Stanford Linear Accelerator Center, Stanford, CA 94309, USA

P. R. Burchat, C. H. Cheng, T. I. Meyer, C. Roat

Stanford University, Stanford, CA 94305-4060, USA

R. Henderson

TRIUMF, Vancouver, BC, Canada V6T 2A3

W. Bugg, H. Cohn

University of Tennessee, Knoxville, TN 37996, USA

J. M. Izen, I. Kitayama, X. C. Lou

University of Texas at Dallas, Richardson, TX 75083, USA

F. Bianchi, M. Bona, D. Gamba

Università di Torino, Dipartimento di Fisica Sperimentale and INFN, I-10125 Torino, Italy

L. Bosisio, G. Della Ricca, S. Dittongo, L. Lanceri, P. Poropat, L. Vitale, G. Vuagnin

Università di Trieste, Dipartimento di Fisica and INFN, I-34127 Trieste, Italy

R. S. Panvini

Vanderbilt University, Nashville, TN 37235, USA

[4]Also with University of California at San Diego, La Jolla, CA 92093, USA

C. M. Brown, P. D. Jackson, R. Kowalewski, J. M. Roney
University of Victoria, Victoria, BC, Canada V8W 3P6

H. R. Band, S. Dasu, M. Datta, A. M. Eichenbaum, H. Hu, J. R. Johnson, R. Liu, F. Di Lodovico, Y. Pan, R. Prepost, I. J. Scott, S. J. Sekula, J. H. von Wimmersperg-Toeller, S. L. Wu, Z. Yu
University of Wisconsin, Madison, WI 53706, USA

T. M. B. Kordich, H. Neal
Yale University, New Haven, CT 06511, USA

1 Introduction

In this paper, we report a preliminary measurement of the $B^0 \to J/\psi\,\pi^+\pi^-$ branching fraction. The motivation for studying these decays comes in part from the possibility of including the $J/\psi\,\rho^0$ mode in the *BABAR* sin2β analysis [1]. It is also expected that due to the Cabibbo and colour suppression of these decays, interference with rare or exotic processes, such as a box diagram containing charged Higgs bosons, could be significant. These effects may appear as deviations of the branching ratio from the Standard Model prediction of $\mathcal{B}(B^0 \to J/\psi\,\pi^+\pi^-) = (4.6 \pm 0.8) \times 10^{-5}$ [2]. The only previous measurement related to this analysis is an upper limit on the $B^0 \to J/\psi\,\rho^0$ branching fraction by CLEO [2], $\mathcal{B}(B^0 \to J/\psi\,\rho^0) < 2.5 \times 10^{-4}$ at 90% confidence level.

The method used is a fit to the distribution of the invariant mass of the two pions, $M(\pi^+\pi^-)$, with the goal of isolating the separate components. Both the $B^0 \to J/\psi\,\rho^0$ and $B^0 \to J/\psi\,\pi^+\pi^-$ (non-resonant) contributions are modelled in the fit function. However, in the present analysis the branching fraction is quoted for the sum of these two modes, as the individual fractions are highly correlated and depend sensitively on model assumptions. The total yield is only sensitive to the normalization of various background sources and so is quite stable. It is expected that separation of the two components will be possible with a considerably larger data set, when a mass dependent angular analysis of the decay products will be possible.

2 The *BABAR* detector and data set

The data used in this analysis were collected with the *BABAR* detector at the PEP-II storage ring. The *BABAR* detector is described in detail elsewhere [3]. Surrounding the beam pipe is a silicon vertex tracker (SVT) to provide precise measurements of positions and angles of charged particles emerging from the interaction region and stand-alone track finding, particularly for particles with momentum below 120 MeV/c. Outside this is a 40-layer drift chamber (DCH) filled with an 80:20 helium-isobutane gas mixture to minimize multiple scattering. The DCH provides measurements of track momenta, as well as energy-loss measurements that contribute to charged particle identification. Surrounding the drift chamber is a novel detector of internally reflected Cherenkov radiation (DIRC) that allows charged hadron identification in the barrel region. Outside the DIRC is a CsI(Tl) electromagnetic calorimeter (EMC), which is used to detect photons and neutral hadrons and to provide electron identification. The EMC is surrounded by a superconducting coil, which provides a magnetic field of 1.5T for momentum measurements. Outside the coil the flux return is instrumented with resistive plate chambers interspersed with iron (IFR) for the identification of muons and long-lived neutral hadrons. The GEANT4 [4] software is used to simulate interactions of particles traversing the *BABAR* detector. A coordinate system is defined with the z axis aligned along that of the detector in the electron beam direction.

The data sample used for the analysis contains approximately 56 million $B\overline{B}$ pairs, corresponding to 51.7 fb^{-1} taken near the $\Upsilon(4S)$ resonance. An additional 6.4 fb^{-1} of data, taken approximately 40 MeV below the $\Upsilon(4S)$ peak, was used in studies of the effect of light $q\overline{q}$ pair backgrounds.

3 Analysis method

3.1 Event selection and B reconstruction

The aim of the event selection is primarily to accept events containing a $B^0 \to J/\psi\,\pi^+\pi^-$ decay while rejecting background both from u, d, s, c quark continuum and $\Upsilon(4S)$ events which do not contain a $B^0 \to J/\psi\,\pi^+\pi^-$ decay.

Events containing $B\overline{B}$ pairs are selected based on track multiplicity and event topology. Tracks in the polar angle region $0.41 < \theta_{\rm lab} < 2.54$ rad, with transverse momentum greater than $100\,{\rm MeV}/c$ are required to pass quality cuts, including number of DCH hits used in the track fit and impact parameters with respect to the nominal beam spot in the $r-\phi$ and $r-z$ planes. At least three tracks must pass the above selection. To reduce continuum background the ratio of second to zeroth Fox-Wolfram moments [5], $R_2 = H_2/H_0$, is required to be less than 0.5. The total charged and neutral energy must be greater than 4.5 GeV in the fiducial region of the detector (charged tracks in the DCH and neutral clusters in the EMC) and the primary vertex of the event must be within 0.5 cm of the average measured beam spot position in the plane transverse to the beamline.

Electron candidates must satisfy the requirement that the ratio of calorimeter energy to track momentum lies in the range $0.75 < E/p < 1.3$, have a cluster shape and size consistent with an electromagnetic shower, and DCH ${\rm d}E/{\rm d}x$ consistent with an electron. If an EMC cluster close to the electron track is consistent with originating from a bremsstrahlung photon, it is added to the electron candidate.

Muon candidates must satisfy requirements on the number of interaction lengths of IFR iron penetrated of $N_\lambda > 2$, the difference in the measured and expected interaction lengths penetrated of $|N_\lambda - N_\lambda^{exp}| < 2$, the position match between the extrapolated DCH track and the IFR hits, and the average and spread of the number of IFR strips hit per layer.

Pion candidates are accepted if they originate from close to the beam spot and fail a charged kaon identification algorithm that is designed to reject pions. The algorithm uses ${\rm d}E/{\rm d}x$ information from the SVT and DCH, and Cherenkov angle and number of photons from the DIRC.

Tracks are required to lie in fiducial ranges within which the efficiency is well known from control samples and the material in the detector is accurately modelled in the simulation. The accepted ranges in laboratory polar angle are $0.41 < \theta_{\rm lab} < 2.41$ rad for electrons, $0.3 < \theta_{\rm lab} < 2.7$ rad for muons, and $0.35 < \theta_{\rm lab} < 2.5$ rad for pions. These ranges correspond approximately to the geometrical acceptances of the EMC, IFR and DIRC, respectively.

$J/\psi \to e^+e^-$ or $\mu^+\mu^-$ candidates are formed from pairs of identified electrons or muons which are fitted to a common vertex and must lie in the invariant mass interval 2.95 (3.06) to 3.14 GeV/c^2 for the e^+e^- ($\mu^+\mu^-$) channel.

B^0 candidates are formed by combining a J/ψ candidate with pairs of oppositely-charged pion candidates that are fitted to a common vertex. We require that both two-prong vertices coincide spatially by demanding

$$\chi^2_{\psi,\pi\pi} = \Sigma_i \frac{(x^i_\psi - x^i_{\pi\pi})^2}{(\sigma(x^i_\psi)^2 + \sigma(x^i_{\pi\pi})^2)} < 6, \qquad (1)$$

where x^i and $\sigma(x^i)$ are the positions and errors of the vertices in the ith spatial dimension. Further selection requirements for B^0 candidates are made using two kinematical variables: the difference ΔE between the energy of the candidate and the beam energy $E^{\rm cm}_{\rm beam}$ in the center-of-mass frame and the beam-energy substituted mass $m_{\rm ES} = \sqrt{(E^{\rm cm}_{\rm beam})^2 - (p^{\rm cm}_B)^2}$. After applying the loose requirements $5.2 < m_{\rm ES} < 5.3\,{\rm GeV}/c^2$ and $|\Delta E| < 120\,{\rm MeV}$, if more than one B^0 candidate re-

mains in the same event only the candidate with the smallest $|\Delta E|$ is kept. Those candidates with $|m_{\rm ES} - 5279.0| < 9.9\,{\rm MeV}/c^2$ and $|\Delta E| < 39\,{\rm MeV}$ form the final signal sample. These ranges correspond to 3σ in the expected resolutions for $m_{\rm ES}$ and ΔE. After all selection criteria have been applied, there are 212 events remaining.

3.2 Fitting to the $\pi^+\pi^-$ mass spectrum

An unbinned, extended maximum likelihood fit is performed on the invariant mass distribution of the two pions for selected events. We consider five categories of events:

- $B^0 \to J/\psi\,\pi^+\pi^-$ (non-resonant) events
- $B^0 \to J/\psi\,\rho^0$ events
- $B^0 \to J/\psi\,K^0_S(K^0_S \to \pi^+\pi^-)$ events
- Background from events with a fake J/ψ
- Inclusive-J/ψ background (that originating from events containing a real J/ψ)

A probability density function (PDF) is constructed for each of these five cases. The total PDF is then formed from the sum of the five PDFs and fitted to the data. The $B^0 \to J/\psi\,K^0_S$ mode is not considered signal for the purposes of determining the branching fraction $B^0 \to J/\psi\,\pi^+\pi^-$.

3.2.1 The signal and K^0_S PDFs

The PDF used to model the $B^0 \to J/\psi\,\pi^+\pi^-$ (non-resonant) mode is the two-body phase space distribution of the pion pair and is given by

$$F_{n.r.}(m) = (m - M_{on})^A \times (M_{off} - m)^B, \tag{2}$$

where the kinematic limits are $M_{on} = 2M_\pi$ and $M_{off} = M_{B^0} - M_{J/\psi}$. The parameters A, B are determined by fitting to the $M(\pi^+\pi^-)$ distribution in simulated $B^0 \to J/\psi\,\pi^+\pi^-$ (non-resonant) events.

The PDF used to model the $B^0 \to J/\psi\,\rho^0$ mode is a relativistic p-wave Breit-Wigner [7] function multiplied by the phase-space shape described above. The ρ^0 mass and width for the Breit-Wigner are fixed to their PDG values [6].

The $B^0 \to J/\psi\,K^0_S$ two-pion invariant mass distribution is modelled by a single Gaussian function with the mass and width fixed to values obtained by fitting a sample of simulated $J/\psi\,K^0_S$ events.

3.2.2 The background PDFs

The $M(\pi^+\pi^-)$ distribution for events without a real J/ψ is derived from a fake-J/ψ sample from data. The sample is selected as in Sec. 3.1 except that at least one of the lepton candidates must fail the appropriate particle identification requirements, thus providing a high statistics data set that models the shape of the non-J/ψ background. In addition the final kinematic requirements are relaxed to $5.2 < m_{\rm ES} < 5.3\,{\rm GeV}/c^2$ and $|\Delta E| < 120\,{\rm MeV}$, which further enlarges the sample. A Monte Carlo study confirms that the $M(\pi^+\pi^-)$ distribution obtained with this procedure correctly describes the shape of the non-J/ψ background. The resulting distribution is parameterized using the sum of two Weibull functions (see Eq. 3) and a Breit-Wigner.

The $M(\pi^+\pi^-)$ background shape from events containing a real J/ψ is obtained with a sample of simulated $B \to J/\psi\, X$ events equivalent to a luminosity of $81\,\mathrm{fb}^{-1}$. Events where the system X is $\pi^+\pi^-$ (non-resonant), ρ^0 or K^0_S $(\pi^+\pi^-)$ are removed from the sample. The resulting shape is well described by a Weibull function [8]:

$$\begin{aligned} F_{J/\psi X}(m) &= C\,V\,(m - M_{on})^{(C-1)} \times \exp[-V(m - M_{max})^C] \\ V &= (C-1)/(C(M_{max} - M_{on})^C), \end{aligned} \tag{3}$$

where M_{max} (the peak position) and C are determined from the fit to the simulated events and M_{on} is the kinematic limit as described above.

3.2.3 Background normalization

The normalization of the background components is obtained from control samples in data. The level of non-J/ψ background is obtained from the data J/ψ-sideband sample. This sample is selected by accepting only events where the $J/\psi \to e^+e^-$ candidate lies in the invariant mass region 3.156 to $3.300\,\mathrm{GeV}/c^2$ or the $J/\psi \to \mu^+\mu^-$ candidate lies in the region 2.980 to $3.024\,\mathrm{GeV}/c^2$ or 3.156 to $3.300\,\mathrm{GeV}/c^2$. The m_{ES} distribution is fit to an ARGUS function [9] for B candidates in which the $J/\psi \to e^+e^-$ or $J/\psi \to \mu^+\mu^-$ candidate lies in the J/ψ sideband. The fit is done separately for e^+e^- and $\mu^+\mu^-$ candidates to obtain the number of background events passing the final kinematic selection in each case. These numbers are then reweighted to make them correspond to the fitted level of background in the $M(e^+e^-)$ or $M(\mu^+\mu^-)$ distribution in the J/ψ mass interval.

The normalization of inclusive-J/ψ background is obtained from the distribution of m_{ES} for events in the ΔE signal region. The m_{ES} distribution is parameterized by a Gaussian (to represent signal and peaking background) and an ARGUS function, which has one shape parameter and an endpoint fixed by the average beam energy in the center-of-mass frame. The peaking background is defined as that which accumulates at $m_{ES} = 5.279$ GeV/c^2. It originates from $B \to J/\psi\, X$ decays such as $B \to J/\psi\, K^*$. The non-peaking component of the inclusive-J/ψ background comes from subtracting the non-J/ψ contribution, on the basis of the scaled sideband events described above, from the total ARGUS background in data. We then add a peaking component, which is obtained from the Gaussian part of the m_{ES} distribution in $B \to J/\psi\, X$ simulation (with $X = \pi^+\pi^-$ (non-resonant), ρ^0 and $K^0_S(\pi^+\pi^-)$ removed). The total background from events containing a real J/ψ is then the sum of peaking and non-peaking components. The peaking component comprises only 5% of the total background. Thus any associated uncertainties, such as those on the branching ratios used in the $J/\psi\, X$ simulation, will have a relatively small effect on the final systematic error.

3.3 Branching fraction determination

The branching fraction is obtained from

$$\mathcal{B}(B^0 \to J/\psi\,\pi^+\pi^-) = \frac{N_{\pi\pi}}{N_{B^0} \times \epsilon_{\pi\pi} \times \mathcal{B}(J/\psi \to \ell^+\ell^-)}, \tag{4}$$

where $N_{\pi\pi}$ is the yield of resonant and non-resonant components obtained from the fit, N_{B^0} is the total number of B^0 and $\overline{B}^0$ in the data sample [10] and $\epsilon_{\pi\pi}$ is the signal efficiency. The J/ψ branching fraction $\mathcal{B}(J/\psi \to \ell^+\ell^-)$ is fixed to the current world average value [6]. We assume that the branching fraction $\Upsilon(4S) \to B^0\overline{B}^0$ is 50%.

The signal efficiency in Eq. 4 is derived from simulated signal events. Imperfect modelling of particle identification is corrected by studies of independent control samples derived from data. The lepton and pion particle identification efficiencies are measured in data with control samples of $\mu^+\mu^-\gamma$, $\mu^+\mu^-e^+e^-$, e^+e^-, $e^+e^-\gamma$, $D^{*+} \to D^0\pi^+$ ($D^0 \to K^-\pi^+$) and $K^0_S \to \pi^+\,\pi^-$. The efficiencies are determined as a function of momentum, and polar and azimuthal angle. We find $\epsilon(J/\psi\,\rho^0) = (27.0 \pm 0.3)\%$, $\epsilon(J/\psi\,\pi^+\pi^-$, non-resonant$) = (26.5 \pm 0.3)\%$ and $\epsilon(J/\psi\,K^0_S) = (2.31 \pm 0.06)\%$. The final corrected signal efficiency is taken as the average of the $J/\psi\,\rho^0$ and $J/\psi\,\pi^+\pi^-$ (non-resonant) efficiencies and is found to be $(26.8 \pm 0.2)\%$, where the error is from Monte Carlo statistics.

4 Results

The full model for the $M(\pi^+\pi^-)$ mass distribution is obtained by summing the five PDFs described in sections 3.2.1 and 3.2.2. A likelihood fit is performed on the $M(\pi^+\pi^-)$ distribution in data with the normalization of the non-J/ψ background fixed to 36.9 events and the inclusive-J/ψ background to 55.1. Thus the only parameters that are allowed to float in the fit are the numbers of $J/\psi\,\pi^+\pi^-$ (non-resonant), $J/\psi\,\rho^0$ and $J/\psi\,K^0_S$ events. The result of the fit is shown in Fig. 1 where the data has been binned and overlayed. The χ^2 of the curve and the data as binned in Fig. 1 is 40.9 for 38 data points. The fit finds $N_{\pi\pi} = 89.9 \pm 13.3$ events, where 43.3 ± 12.7 are included in the ρ^0

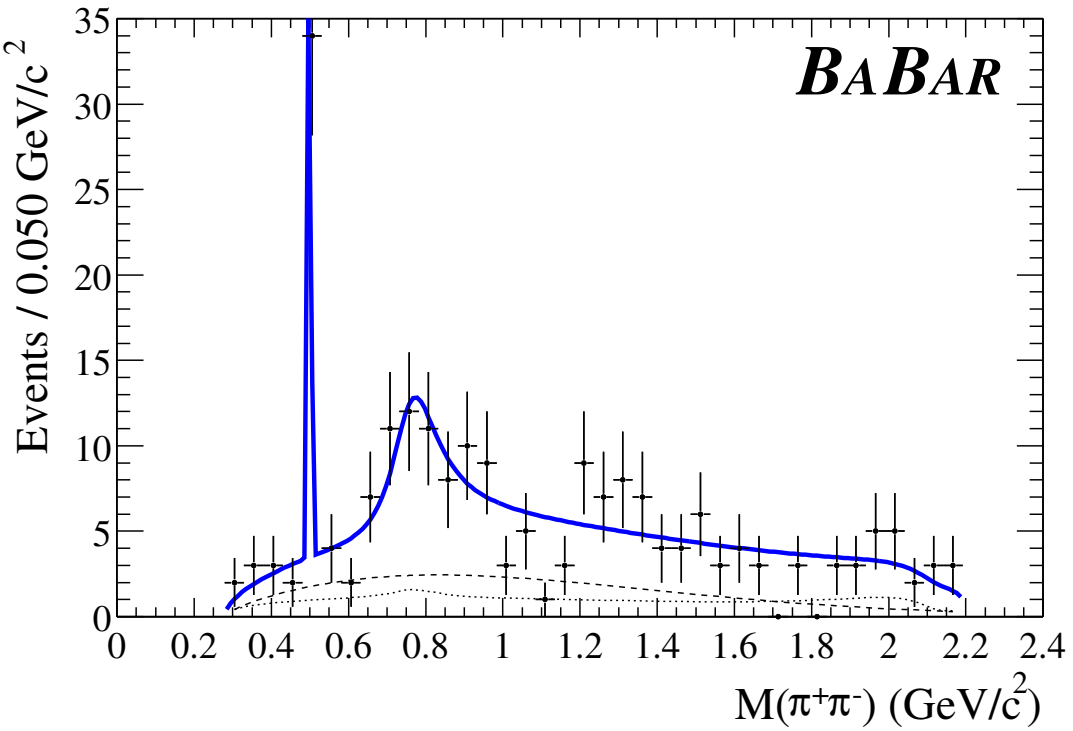

Figure 1: Distribution of the invariant mass M$(\pi^+\pi^-)$ for events passing all selection criteria. The solid line is the result of the unbinned likelihood fit. The dotted (dashed) line represents the background from non-J/ψ (inclusive-J/ψ) events.

component and 46.6 ± 14.5 are included in the non-resonant component. The number of events in

Table 1: Number of events for each signal and background category floated in the fit. $J/\psi\,\pi^+\pi^-$(counting) is the $J/\psi\,\pi^+\pi^-$ yield determined by counting the number of events that pass all selection criteria and subtracting the background and K^0_S estimates from it, as described in Sec. 6.

B decay mode	Yield
$J/\psi\,\rho^0$	43 ± 13
$J/\psi\,\pi^+\pi^-$ (non-resonant)	47 ± 15
$J/\psi\,K^0_S(K^0_S \to \pi^+\pi^-)$	29 ± 6
$J/\psi\,\pi^+\pi^-$ (fit)	90 ± 13
$J/\psi\,\pi^+\pi^-$ (counting)	91 ± 17

the K^0_S component is 29.0 ± 5.5. Inserting the result into Eq. 4 yields the branching ratio

$$\mathcal{B}(B^0 \to J/\psi\,\pi^+\pi^-) = (5.0 \pm 0.7) \times 10^{-5},$$

where the error is statistical. The results are summarised in Table 1.

5 Systematics studies

The systematic errors on the final branching fraction measurement arise from uncertainties in the signal efficiency, fitted yield, number of $B\overline{B}$ pairs produced and $J/\psi \to \ell^+\ell^-$ branching fraction. $N_{B\overline{B}}$ is known to 1.1% with the dominant contribution to the uncertainty coming from the error on the efficiency of the B-counting selection. $\mathcal{B}(J/\psi \to \ell^+\ell^-)$ is known to 1.7% [6].

The uncertainty on the pion particle identification efficiency is 2.5% per pion. This is determined in part by the limited number of events in the control sample. Other contributions are from applying different techniques to deduce the kaon contamination in the control sample and deviations between the efficiency for pions in the control sample and in the $J/\psi\,\pi^+\pi^-$ sample. Thus the final systematic error from pion identification is 5%. Uncertainties on electron and muon particle identification efficiencies come from studies of yields in $B \to J/\psi\,X$ data events and give an error of 1.3%. The total systematic error on particle identification efficiency is then 5.2%.

The uncertainty in the determination of the tracking efficiency is 1.3% per track, which sums coherently for the four tracks coming from the B^0.

The efficiency of the convergence requirement on the $\pi^+\pi^-$ vertex fit has been studied with a sample of $\psi(2S) \to \ell^+\ell^-$ decays. Data and simulation are found to be in good agreement with an associated systematic error of 1%.

The $J/\psi\,\rho^0$ component of the final sample will introduce an uncertainty on efficiency due to the unknown polarisation of the ρ. Studies of efficiency variations between samples of simulated events with longitudinal and transverse polarisations lead to a systematic error estimate of 2.5%.

To account for imperfect simulation of selection variables, the requirements on J/ψ invariant mass, $\chi^2_{\psi,\pi\pi}$ and $|\Delta E|$ are varied within reasonable limits, and the analysis is repeated for each selection. The deviation of the efficiency-corrected yield from the fit, in each case, is assigned as a systematic error. Varying the size of the J/ψ mass interval by $\pm 14\,\mathrm{MeV}/c^2$ and the $|\Delta E|$ requirement by $\pm 1\sigma$, where $\sigma = 13\,\mathrm{MeV}$ is the standard deviation observed in data, shows variation at the level

Table 2: Summary of the systematic errors for $\mathcal{B}(B^0 \to J/\psi\,\pi^+\pi^-)$.

Source of Uncertainty	Systematic Error
B-Counting	1.1%
$\sigma(\mathcal{B}(J/\psi \to \ell^+\ell^-))$	1.7%
PID efficiencies	5.2%
Track efficiencies	5.2%
$\pi\pi$ vertex efficiency	1.0%
ρ^0 polarisation	2.5%
Selection variation	7.1%
PDF parameter variation	4.9%
Simulation statistics	0.7%
Total	11.8%

of 0.4% and 6.8%, respectively. The $\chi^2_{\psi,\pi\pi}$ requirement is varied between 3 and 9 yielding an error of 2.1%. These errors are added in quadrature to give the total systematic uncertainty due to modelling of the selection requirements.

To assess the effect of the chosen signal and background shapes on the fitted yields, the fixed parameters of these PDFs are varied within their statistical errors, allowing for correlations. This produces a total systematic error due to fit parameter variation of 4.9%. The total systematic uncertainty from all sources is found to be 11.8%, as summarized in Table 2.

6 Cross checks

The fit was repeated using a simple Breit-Wigner (non-relativistic, width independent of mass) for the ρ^0 lineshape. While the $J/\psi\,\rho^0$ yield decreased by 23% and that for $J/\psi\,\pi^+\pi^-$ (non-resonant) increased by 27%, the total $J/\psi\,\pi^+\pi^-$ yield increased by less than 1%. This check is also equivalent to varying the parametrization for $J/\psi\,\pi^+\pi^-$ (non-resonant) and is strictly a test of the stability of the total $J/\psi\,\pi^+\pi^-$ yield. It should be noted that the simple Breit-Wigner is technically the wrong shape to use for the ρ^0 parametrization.

Another way to model the backgrounds is to use a smoothing algorithm on the data rather than impose definite PDF shapes. The chosen method creates a Gaussian kernel for each event in order to build a shape that describes the input data [11]. The resulting PDF follows fluctuations in the input data as accurately as possible and checks how strongly the fitted signal yield depends on the chosen method of background parameterization. Changing the background modelling in this way alters the total fitted yield by less than one event.

The signal yield can also be calculated by counting the number of data events passing all the cuts and subtracting the estimated numbers of background and $J/\psi\,K^0_S$ events. This method gives 91.0 ± 16.6 $J/\psi\,\pi^+\pi^-$ events, to be compared to the 89.9 ± 13.3 given by the fit to the $M(\pi^+\pi^-)$ distribution.

There are 43.3 ± 12.7 events in the ρ^0 resonance component. On the assumption that the non-ρ^0 signal component is well modelled by $J/\psi\,\pi^+\pi^-$ phase space, we measure $\mathcal{B}(B^0 \to J/\psi\,\rho^0) = (2.4 \pm 0.7) \times 10^{-5}$, where the error is statistical only.

7 Conclusion

In summary, we have measured the branching fraction for B^0 meson decay to the final state $J/\psi\,\pi^+\pi^-$ to be $(5.0 \pm 0.7\,(\text{stat}) \pm 0.6\,(\text{syst})) \times 10^{-5}$. The technique of fitting the mass spectrum of the $\pi\pi$ system will become important for future measurements in this channel, particularly as it will provide separation between the resonant and non-resonant components given a larger data set. It is important to reliably isolate the $J/\psi\,\rho^0$ component in order to contribute to a measurement of the Unitarity Triangle angle β.

8 Acknowledgments

We are grateful for the extraordinary contributions of our PEP-II colleagues in achieving the excellent luminosity and machine conditions that have made this work possible. The success of this project also relies critically on the expertise and dedication of the computing organizations that support *BABAR*. The collaborating institutions wish to thank SLAC for its support and the kind hospitality extended to them. This work is supported by the US Department of Energy and National Science Foundation, the Natural Sciences and Engineering Research Council (Canada), Institute of High Energy Physics (China), the Commissariat à l'Energie Atomique and Institut National de Physique Nucléaire et de Physique des Particules (France), the Bundesministerium für Bildung und Forschung (Germany), the Istituto Nazionale di Fisica Nucleare (Italy), the Research Council of Norway, the Ministry of Science and Technology of the Russian Federation, and the Particle Physics and Astronomy Research Council (United Kingdom). Individuals have received support from the A. P. Sloan Foundation, the Research Corporation, and the Alexander von Humboldt Foundation.

References

[1] BABAR Collaboration, B. Aubert *et al.*, hep-ex/0203007, presented at La Thuile 2002.
BABAR Collaboration, B. Aubert *et al.*, Phys. Rev. Lett. **87**, 091801 (2001).
BABAR Collaboration, B. Aubert *et al.*, hep-ex/0201020, submitted to Phys. Rev. D.

[2] CLEO Collaboration, M. Bishai *et al.*, Phys. Lett. B **369**, 186 (1996).
Eq. 1 is used to estimate both the Standard Model prediction for $\mathcal{B}(B^0 \to J/\psi\,\rho^0)$ and that for $\mathcal{B}(B^0 \to J/\psi\,\pi^+\pi^-)$ (non-resonant), where the factor of 0.5 is excluded from the latter calculation. The sum of the two results gives the prediction for $\mathcal{B}(B^0 \to J/\psi\,\pi^+\pi^-)$.

[3] BABAR Collaboration, B. Aubert *et al.*, Nucl. Instr. and Meth. **A479**, 1 (2002).

[4] http://wwwinfo.cern.ch/asd/geant4/geant4.html

[5] G. C. Fox and S. Wolfram, Nucl. Phys. B **149**, 413 (1979).

[6] Particle Data Group Collaboration, D. E. Groom *et al.*, Eur. Phys. J. C **15**, 1 (2000).

[7] J. D. Jackson, Nuovo Cim. **34**, 1644 (1964).

[8] http://www.weibull.com/LifeDataWeb/the_weibull_distribution.htm

[9] ARGUS Collaboration, H. Albrecht *et al.*, Z. Phys. C **48**, 543 (1990).

[10] For a description of the B counting analysis see for example section VI of BABAR Collaboration, B. Aubert *et al.*, Phys. Rev. D **65**, 032001 (2002).

[11] K. S. Cranmer, ALEPH 99-144 (1999).
http://www-wisconsin.cern.ch/~cranmer/keys.html.